HHS Public Access

Author manuscript

Angiogenesis. Author manuscript; available in PMC 2020 August 01.

Published in final edited form as:

Angiogenesis. 2019 August ; 22(3): 369–382. doi:10.1007/s10456-019-09662-4.

Anti-Secretogranin III Therapy of Oxygen-Induced Retinopathy with Optimal Safety

Fen Tang[1,2], **Michelle E. LeBlanc**[1], **Weiwen Wang**[1], **Dan Liang**[2], **Ping Chen**[1,3], **Tsung-Han Chou**[1], **Hong Tian**[4], **Wei Li**[1]

[1]Bascom Palmer Eye Institute, Department of Ophthalmology, University of Miami School of Medicine, Miami, Florida, USA.

[2]State Key Laboratory of Ophthalmology, Zhongshan Ophthalmic Center, Sun Yat-Sen University, Guangzhou, China.

[3]Department of Ophthalmology, Renji Hospital of Shanghai Jiaotong University, Shanghai, China.

[4]Everglades Biopharma, LLC, Miami, Florida, USA.

Abstract

Retinopathy of Prematurity (ROP) with pathological retinal neovascularization is the most common cause of blindness in children. ROP is currently treated with laser therapy or cryotherapy, both of which may adversely affect the peripheral vision with limited efficacy. Owing to the susceptibility of the developing retina and vasculatures to pharmacological intervention, there is currently no approved drug therapy for ROP in preterm infants. Secretogranin III (Scg3) was recently discovered as a highly disease-restricted angiogenic factor, and a Scg3-neutralizing monoclonal antibody (mAb) was reported with high efficacy to alleviate oxygen-induced retinopathy (OIR) in mice, a surrogate model of ROP. Herein we independently investigated the efficacy of anti-Scg3 mAb in OIR mice and characterized its safety in neonatal mice. We developed a new Scg3-neutralizing mAb recognizing a distinct epitope and independently established the therapeutic activity of anti-Scg3 therapy to alleviate OIR-induced pathological retinal neovascularization in mice. Importantly, anti-Scg3 mAb showed no detectable adverse effects on electroretinography and developing retinal vasculature. Furthermore, systemic anti-Scg3 mAb induced no renal tubular injury or abnormality in kidney vessel development and body weight gain of neonatal mice. In contrast, anti-vascular endothelial growth factor drug aflibercept showed significant side effects in neonatal mice. These results suggest that anti-Scg3 mAb may have the safety and efficacy profiles required for ROP therapy.

Keywords

Secretogranin III; Scg3; angiogenic factor; anti-angiogenic therapy; oxygen-induced retinopathy; retinopathy of prematurity

Correspondence to Wei Li, w.li@med.miami.edu; Tel: +1-305-326-6445; Fax: +1-305-547-3658.

Conflict of Interest

M.E.L, H.T. and W.L. are shareholders of Everglades Biopharma, LLC and/or LigandomicsRx, LLC. M.E.L., W.W. and W.L. are inventors of pending patents.

Introduction

To date, nearly all conventional angiogenic factors are discovered based on their functional activity on normal vessels and subsequently characterized for their involvement in disease pathogenesis. Therapies targeting these conventional angiogenic factors may inhibit both pathological and physiological angiogenesis. This is highlighted by anti-vascular endothelial growth factor (VEGF) drug bevacizumab that exerts not only therapeutic inhibition on cancer vessels but also adverse side effects on normal vasculatures [1]. The lack of disease selectivity is particularly a safety concern for anti-angiogenic therapy of neonatal diseases, in which premature vasculatures are highly susceptible to angiogenesis inhibition.

Retinopathy of prematurity (ROP) with pathological retinal neovascularization (RNV) is the most common cause of vision loss in children [2]. The disease primarily affects preterm infants weighing 1,250 grams or less, or born before 31 weeks of gestation. About 28,000 of newborn babies in the U.S. fall into this category annually, and of these 14,000 – 16,000 are afflicted by ROP [3]. The disease may progress toward partial or complete retinal detachment with severe vision loss and even blindness [2].

ROP is currently treated with laser therapy or cryotherapy, both of which destroy the peripheral vision to save the central vision with limited efficacy and do not address the underlying cause of pathological RNV [2, 4]. The advent of VEGF inhibitors, such as ranibizumab and aflibercept, is a major breakthrough for pharmacological therapy of adult ocular vascular diseases, such as neovascular age-related macular degeneration (AMD) and diabetic retinopathy [5]. Although clinical studies showed limited efficacy of anti-VEGF drugs to treat ROP [6–8], bevacizumab and ranibizumab caused adverse side effects in ROP infants [9, 10]. Aflibercept was also associated with retinal and vascular adverse effects in neonatal mice and dogs [11, 12]. Consequently, no drug has been approved for ROP.

We recently discovered secretogranin III (Scg3) as a highly disease-selective angiogenic factor by comparative ligandomics [13]. Scg3 preferentially bound to and stimulated angiogenesis of diseased but not normal vessels, whereas VEGF bound to and promoted angiogenesis of both diseased and healthy vessels [13]. Furthermore, we developed anti-Scg3 ML49.3 monoclonal antibody (mAb) and demonstrated its high efficacy to alleviate oxygen-induced retinopathy (OIR), a surrogate animal model of ROP [13, 14].

In this study, we characterized ML49.3 and ML78.2 mAbs as two non-competing Scg3-neutralizing antibodies and independently established Scg3 as a therapeutic target by demonstrating the therapeutic activity of ML78.2 mAb to inhibit OIR-induced pathological RNV. More importantly, our data showed that anti-Scg3 mAb has minimal adverse side effects on the developing retina and other organs. These results suggest that anti-Scg3 mAbs with high disease selectivity represent a new class of selective angiogenesis blockers that may have the safety and efficacy profiles required to treat ROP.

Materials and methods

Animals

C57BL/6J mice and NOD *scid* gamma (NSG) mice were purchased from the Jackson Laboratory. All animal experimental procedures were approved by the Institutional Animal Care and Use Committee (IACUC) at University of Miami. All organs were isolated after euthanasia.

Anti-Scg3 monoclonal antibodies

Seven clones of anti-Scg3 mAbs, including ML7.1, ML16, ML 49.3, ML78.2, ML153.2, ML162.1 and ML190.2, were generated and sequenced, as described [13, 15]. Hybridomas were cultured in RPMI 1640 medium supplemented with 10% fetal bovine serum (FBS), 1x GlutaMAX and 1x pen/strep, and gradually adapted to Hybridoma-SFM medium (Thermo Fisher). mAbs were purified from serum-free conditioned medium using protein G columns [16]. Alternatively, ML78.2 mAb was purified from ascites of NGS immunodeficient mice (male and female) in a large quantity for *in vivo* studies, as described [17]. Ascites were harvested from mice, centrifuged, and filtered, followed by mAb purification as above. Purified mAb was washed with phosphate-buffered saline (PBS) in filter spin units (Millopore, 10 kDa cut-off), concentrated and quantified against a standard curve of human IgG (Sigma).

Epitope binning

Human Scg3 (Sino Biological) was labeled with biotin using EZ-Link™ Sulfo-NHS-Biotin labeling reagent (NHS-Biotin, Thermo Fisher) according to the manufacturer's protocol. Briefly, Scg3 in PBS was incubated with NHS-Biotin for 30 min at room temperature, followed by incubation with 1/10 volume of 100 mM Tris-HCl pH 8.0 to stop the reaction. Scg3-biotin was purified using desalt spin columns (Bio-Rad).

Epitope binning was performed to analyze epitope binding specificity of mAbs [18, 19]. In brief, Scg3-biotin was incubated with streptavidin biosensors (Pall ForteBio). After washing, anti-Scg3 mAbs were incubated with Scg3 on biosensors as blocking mAbs, followed by washing and incubation with different anti-Scg3 mAbs using Octet RED96 instrument (Pall ForteBio) to monitor binding kinetics.

scFv

Antibody single-chain variable fragments (scFv) with variable regions of the heavy (VH) and light chains (VL) were generated by PCR using overlapping primers. scFv with a flexible linker (VH-GGGGSGGGGSGGGGS-VL) was cloned into pComb3xSS phagemid vector (Addgene, Cat. #63890) at SfiI sites and verified by DNA sequencing [20]. ML49.3 scFv and ML78.2 scFv with a C-terminal polyhistidine tag and a HA tag were expressed in bacteria and purified using Ni^{2+} columns [21, 22].

ELISA

For ELISA binding competition assay, Scg3 was immobilized on ELISA plates, blocked, and incubated with purified scFv in the presence or absence of excess ML49.3 or ML78.2

mAb. Bound scFv was detected using peroxidase-conjugated anti-HA mAb (Sigma) and colorimetric assay [23].

Neutralization assay

Endothelial cell proliferation assay was carried out as described [13]. Briefly, human umbilical vein endothelial cells (HUVECs) at 4–8 passages were plated in 96-well plates (2×10^3 cells/well). After overnight culture, a quarter of the medium in each well was substituted with conditioned medium of different hybridoma clones or control medium. Cells were cultured for additional 48 h in the presence or absence of Scg3 (1 μg/ml), collected by trypsin digestion, and counted in PBS with 1 mM trypan blue using a hemocytometer.

Anti-angiogenic therapy

C57BL/6J mice (male and female, randomly assigned) were exposed to 75% oxygen at postnatal day 7 (P7) and switched back to room air at P12 to induce OIR [13, 24]. At P14, pups received a single intravitreal injection of aflibercept (2 μg/0.5 μl/eye), anti-Scg3 mAb, control mouse IgG (4 μg/0.5 μl/eye), PBS or non-injection control. Eyes were enucleated from euthanized mice at P17 and fixed in 4% paraformaldehyde for 1 h. Retinas were isolated, stained with Alexa Fluor 488-isolectin B4 (10 μg/ml, Thermo Fisher) overnight at 4°C, and analyzed by confocal microscopy. Neovascularization (i.e., relative fluorescence intensity or pixel), neovascular (NV) tufts, branch points and central avascular area were blind coded and quantified to determine OIR-induced RNV [13, 24]. All data were normalized against non-injection control.

Alternatively, we administered i.p. aflibercept (5 and 10 mg/Kg body weight), anti-Scg3 mAb (10 mg/Kg) or PBS at P14, 16 and 18, and isolated retinas at P19 to analyze OIR-induced RNV as above. Additionally, we injected i.p. aflibercept, anti-Scg3 mAb or PBS at P12, 14, and P16, and harvested retinas at P17 to quantify RNV.

Scotopic Electroretinography (ERGj

C57BL/6J mice (male and female) received intravitreal injection of ML78.2 mAb or aflibercept (4 μg/0.5 μl/eye) in one eye with PBS for the fellow eye at P14. ERG was performed at P21 and P42 to evaluate retinal function. Before ERG, mice were subjected to dark adaptation overnight. Pupils were dilated with sequential application of tropicamide and phenylephrine eyedrops. Anesthetized mice were positioned on a platform with a heating pad to maintain the body temperature at 37°C. Heads were stabilized with mouth bite bar and a nose holder that allowed unobstructed vision, and corneas were moisture with balanced salt solution (BSS) ophthalmic solution.

For ERG, a reference electrode with stainless needle was inserted into skull skin, and ground electrode with stainless needle was placed into tail skin. Two platinum corneal electrodes were laid on the both eyes. ERG was recorded under a scotopic condition using a series of white LED light stimulus with an intensity setting of 5 dB (10.5 Candela/m^2). The number of sweeps was 30, and the time between sweeps was 1 second. Signals were amplified and recorded by a computer. Each mouse was tested 3 times to get an average value. The a-wave

amplitude was measured from baseline to the trough of the a-wave, and the b-wave amplitude was measured from the trough of the a-wave to the peak of the b-wave.

Systematic toxicity

We injected i.p. aflibercept (5 and 10 mg/Kg), anti-Scg3 mAb (10 mg/Kg) or PBS into C57BL/6J mice (male and female) at P1, 3 and 5. Retinas were isolated at P6 and stained with Alexa Fluor 488-isolectin B4 for analysis of the retinal vasculature by confocal microscopy as above [13]. The radius of total retinas and vascularized retinas was measured. Percentage of vascularized retinal area (i.e., vascularized area/total retina area x 100%) was calculated. Vessel density was quantified by Photoshop. The number of branch points was also quantified in a defined area (0.16 mm^2) [13].

Alternatively, mice received aflibercept, anti-Scg3 mAb or PBS at P3, 5, 7, 9, 11 and 13 as above. Body weight was monitored from P1 to P15. Mice were sacrificed at P15. Retinas were isolated, stained with Alexa Fluor 488-isolectin B4 and quantified for vessel density and branch points. Furthermore, kidneys were isolated at P15, fixed overnight and embedded in paraffin.

Histopathology and immunohistochemistry

Kidney sections in 7-μm thickness were deparaffmized [25], heated in Rodent Decloaker solution (Biocare Medical) for 30 min to retrieve antigens, and blocked with 1% BSA and 0.1% Triton-100 in PBS for 1 h. Tissue sections were incubated with FITC- or Alexa Fluor 594-labeled anti-CD31 mAb (Biolegend) at 4°C overnight. Nuclei were stained with DAPI. Tissue sections were analyzed under an AxioImager fluorescence microscope (Carl Zeiss). Furthermore, tissue sections were stained with hematoxylin and eosin (H&E) for structural examination using a light microscope.

Tubular injury was evaluated in each viewing field. Tubular injury was defined as tubular dilatation, tubular atrophy and vacuolization. Briefly, only cortical tubules were quantified with the following scoring system: 0 = no tubular injury; 1 = <10% of tubules injured; 2 = 10–25% of tubules injured; 3 = 26–50% of tubules injured; 4 = 51–75% of tubules injured; 5 = >75% of tubules injured [26]. The size of individual glomeruli was calculated as the average of the largest and smallest glomerular diameters within viewing fields [27]. Vessel density was quantified using Photoshop [13].

Statistical analysis

Data are expressed as mean ± SEM and analyzed using one-ANOVA test or Student's t-test. Data are considered significant when $p<0.05$.

Results

Non-competing Scg3-neutralizing mAbs

We developed seven clones of anti-Scg3 mAbs (Fig. 1A), including Scg3-neutralizing ML49.3 mAb that was characterized in a recent study [13]. Antibody sequencing revealed that all seven mAbs are independent clones. Except ML190.2, all other six clones of mAbs

were capable of neutralizing Scg3-induced proliferation of HUVECs (Fig. 1B). Epitope binning analyses revealed that ML49.3 mAb did not compete with all other mAb clones for Scg3 binding and that ML78.2 mAb competed with ML7.1, ML16, ML153.2 and ML162.1 mAbs (Fig. 1C). These results suggest that ML78.2 and ML49.3 mAbs bind to Scg3 non-competitively.

To independently verify these findings, we labeled Scg3-neutralizing mAbs with NHS-Biotin for ELISA competition assay. However, all labeled mAbs lost their Scg3 binding activity, implying that lysine residue(s) in mAbs may be critically important for Scg3 binding. To circumvent the problem, we produced ML49.3 scFv and ML78.2 scFv with an HA tag. ELISA competition assay confirmed that ML49.3 scFv binding to Scg3 was blocked by ML49.3 mAb but not by ML78.2 mAb, and vice versa (Fig. 1D, E). These results confirmed that ML78.2 and ML49.3 recognize different Scg3 epitopes without competition.

Anti-Scg3 therapy through intravitreal administration

Our recent study discovered Scg3 as a novel angiogenic factor and demonstrated high efficacy of anti-Scg3 ML49.3 mAb to alleviate pathological RNV in OIR mice [13]. To independently validate these findings, we characterized the therapeutic activity of non-competing Scg3-neutralizing ML78.2 mAb in OIR mice. OIR induced the central avascular region and peripheral RNV at P17 with increased vessel intensity (i.e., pixel) and NV tufts (Fig. 2A, healthy retina vs. non-injection or PBS) as described [13, 24]. The normal pattern of retinal vasculature was also disrupted with increased branch points. Intravitreal injection of ML78.2 mAb at P14 reduced the intensity of OIR-induced RNV and NV tufts (Fig. 2B, C). The disorganized vasculature was also restored to the normal pattern, as indicated by the quantification of branch points (Fig. 2D). Interestingly, ML78.2 mAb significantly reduced the central avascular region (Fig. 2E). As a positive control, intravitreal aflibercept also significantly inhibited RNV intensity, NV tufts, and branch points (Fig. 2). Aflibercept slightly reduced the central avascular area, albeit without statistical significance (Fig. 2E). Control IgG showed no therapeutic activity.

Anti-Scg3 therapy through intraperitoneal injection

A potential pitfall of OIR therapy is that intravitreal injection into small mouse eyes at P14 may increase intraocular pressure (IOP), thereby disrupting pathological RNV [11]. This concern was partially alleviated by the inclusion of control groups, such as PBS or control IgG with all data normalized against non-injection controls. Nonetheless, we investigated the therapeutic activity of ML78.2 mAb through i.p. administration to circumvent potential artifacts associated with intravitreal injection. ML78.2 mAb injected i.p. at P14, 16 and 18 significantly inhibited OIR-induced RNV analyzed at P19, including vessel intensity, NV tufts and branch points (Fig. 3). Likewise, aflibercept injected i.p. in the similar therapeutic scheme also ameliorated RNV.

The above therapies were to treat OIR at P14 or 2 days after mice were switched from 75% oxygen to room air to induce OIR. We also investigated the potential of systemic anti-Scg3 therapy to prevent OIR onset by starting the therapy at P12 when OIR was induced. We inj

ected therapeutic agents at P12, P14 and P16, and analyzed RNV at P17. The results showed that both anti-Scg3 ML78.2 mAb and aflibercept prevented OIR-induced RNV, NV tufts and branch points with similar results to the therapies started at P14 (Supplementary Fig. 1).

Adverse effects on retinal function

Previous studies reported that anti-VEGF drugs induce adverse effects in preterm ROP infants or neonatal animals [9, 11, 12]. Because of Scg3 disease selectivity, we predicted that anti-Scg3 mAb may have optimal safety in neonatal mice. To investigate adverse effects of anti-Scg3 mAb on retinogenesis, mice received intravitreal anti-Scg3 mAb at P14 were characterized for retinal function of ERG at P21 and P42. The results showed that ML78.2 mAb did not alter the amplitude and latency of a- or b-wave at P21 (not shown) or P42 (Fig. 4B-F). Aflibercept reduced the amplitudes of a- and b-waves at P21, albeit without statistical significance (not shown). This trend continued to increase at P42 with a significant reduction of b-wave amplitude at P42 ($p<0.05$, Fig. 4A,E), consistent with a previous study [11]. No latency was altered by aflibercept at P21 (not shown) or P42 (Fig. 4D, F). These findings suggest that VEGF inhibitors may affect retinal development with long-term adverse effects on retinal function and that anti-Scg3 mAb shows no such impairment.

Adverse effects on retinal vascular development

Mouse retinal superficial plexus starts to form at birth, spreading from the optical nerve head toward the peripheral of the retina until P8 [28]. Deep plexus develops from P7-P12, followed by the formation of intermediate plexus from P14-P21. Compared to anti-VEGF drugs, one of the important advantage of anti-Scg3 therapy is its high disease selectivity [13]. Thus, we predicted that anti-Scg3 mAb should have minimal adverse effects on retinal vascular development. We injected i.p. ML78.2 mAb, aflibercept or PBS as early as P1 to circumvent intravitreal injection-related disturbance and isolated the whole retina at P6. Blood vessels of flat-mount retinas were stained with Alexa Fluor 488-isolectin B4. The vascularized area was compared to the total retinal area. The results showed that aflibercept significantly inhibited the retinal vascularization as quantified by the percentage of vascularized area, radius of vascularized area, vessel intensity, and branch points (Fig. 5). These results are consistent with severe defect of $VEGF^{-/+}$ mice in vasculogenesis and normal phenotype of $Scg3^{-/-}$ mice [29, 30].

Furthermore, retina vascularization was assessed at P15 (Supplementary Fig. 2). Similar to the results at P6, anti-Scg3 mAb had no detrimental effect on retinal vascular development at P15. By contrast, aflibercept significantly reduced vessel density and branch points.

Systemic adverse effects on body weight gain

Previous studies indicated that intravitreally-injected bevacizumab can escape from the eye into the systemic circulation [31, 32]. It was speculated that leaked anti-VEGF drugs in ROP infants has the potential to cause deleterious effects on developing organs, vasculatures and neurons [33, 34]. To directly investigate systemic adverse effects, we injected i.p. anti-Scg3 mAb, aflibercept or PBS into neonatal mice every other day, starting at P3. Aflibercept caused significant retardation in body weight gain in a dose-dependent manner (Fig. 6A, B). Additionally, two mice in high-dose group (3 mice/group) and one mouse in low-dose group

died at P15. By contrast, no untoward effect on body weight gain was observed for ML78.2 mAb (Fig. 6A, C).

Renal toxicity

To investigate potential effects of anti-Scg3 therapies on the developing kidney, we administered i.p. aflibercept and anti-Scg3 mAb as in the body weight study above. H&E staining revealed that aflibercept induced tubular dilatation at P15 (Fig. 7A, top panel, and 7B), similar to renal cysts with dilated tubules in neonatal mice treated with VEGF receptor 2 (VEGFR2) inhibitor [35]. The glomeruli were significantly enlarged (Fig. 7A, top panel, and 7C). In contrast, mice treated with ML78.2 mAb appeared to have normal kidney structure.

To analyze the vascular development, endothelial cells in kidney sections were labeled with FITC-conjugated anti-CD31 mAb. The results showed marked loss of FITC-CD31-positive endothelial cells in the kidney treated with aflibercept, but not anti-Scg3 mAb (Fig. 7A, middle panel). These results were confirmed using Alexa Fluor 594-anti-CD31 Ab (Fig. 7A, bottom panel, and 7D). These findings suggest that anti-Scg3 therapy is highly safe to the developing kidney.

Discussion

Scg3 was recently discovered as a novel angiogenic factor, and anti-Scg3 polyclonal antibodies (pAbs) and ML49.3 mAb were characterized for anti-angiogenic therapy of OIR and diabetic retinopathy with high efficacy [13]. Given that Scg3 is a newly-identified angiogenic factor, it is important to independently validate its therapeutic potential. This study characterized ML78.2 and ML49.3 mAbs as two non-competing Scg3-neutralizing antibodies. In contrast to pAbs with possible off-target effects, mAbs minimally cross-react with other proteins and are well recognized as selective reagents for target validation as well as therapy. Therefore, demonstration of ML78.2 and ML49.3 mAb to ameliorate OIR-induced RNV in mice with high efficacy in this and previous studies independently supports Scg3 as a bona fide target for anti-angiogenic therapy [13].

Although intravitreal ML78.2 mAb reduced avascular area in the central retina (Fig. 2E), this effect was not observed for the same mAb through intraperitoneal injection (data not shown) or for intravitreal ML49.3 mAb in our recent study [13]. Aflibercept had no significant effect on the avascular region in all cases in this study. Interestingly, a previous report showed that aflibercept increased avascularization in the central retina of OIR mice [11]. Therefore, additional studies are needed to characterize the effects of anti-Scg3 mAb and aflibercept on the avascular area in OIR mice.

Compared to wet AMD, a daunting challenge to develop therapeutic drugs for ROP is rigorous safety requirements. In general, AMD patients in the later lifespan require therapies with minimal adverse effects only for a few years. Similarly, toxicity tolerance threshold for anti-angiogenic therapy of cancer could be set at a relatively high level, even with some severe or fatal adverse effects as reported for bevacizumab [1]. In contrast, drug therapies for ROP infants should have not only short-term safety but also minimal long-term adverse

impact on their future learning activities, career development and quality of life. In this regard, the number one priority of developing drug therapies for ROP is stringent safety requirements. On the other hand, unlike adults, preterm infants with developing vasculatures, neural circuits and organs are particularly susceptible to pharmacological interventions that may disrupt or interfere with normal vasculogenesis, retinogenesis and other organogenesis. The dichotomy between stringent safety requirements and developmental vulnerability confers difficulties in ROP drug therapy. Consequently, no drug has been approved for ROP.

VEGF is not only an angiogenic factor critical for vasculogenesis but also a neurotrophic factor that may play an important role in retinogenesis [29, 36]. Thus, blockade of VEGF may adversely affect vascular and neural development. This notion is supported by the severe defects of vasculogenesis in $VEGF^{-/+}$ mice that die in utero [29]. Indeed, a clinical study indicated that significant vascular and macular abnormalities in ROP eyes treated with bevacizumab [9]. Anti-VEGF therapy in other clinical studies and case reports of ROP was also associated with serious adverse outcomes [10, 37–39]. Intravitreal aflibercept in neonatal dogs inhibited retinal vascular development [12]. Furthermore, intravitreal injection of aflibercept at P14 in OIR mice resulted in significant reduction of ERG b-wave amplitude at P21 and P42 days [11]. Our results also indicated that aflibercept intravitreally injected at P14 markedly suppressed b-wave amplitude at P42 (Fig. 4). On the other hand, clinical studies indicated that VEGF inhibitors alleviated ROP only with limited efficacy [6, 7, 40, 41]. As a result, no anti-VEGF drug has been approved for ROP therapy.

A new trend to reduce adverse effects is to develop novel targeted therapies against disease-selective angiogenic receptors and ligands. One of the examples is prion-like protein doppel specifically expressed on the surface of tumor endothelial cells [42]. Doppel promoted tumor angiogenesis by activating VEGF receptor 2 (VEGFR2). Doppel-binding glycosaminoglycan selectively targeted tumor angiogenesis but spared normal vasculatures. The drawback is that the glycosaminoglycan targeting VEGFR2 via doppel may not circumvent cancer resistance to anti-VEGF therapies.

Another example of attempting to develop disease-selective anti-angiogenic therapy is the inhibitors against CCR3 receptor, which is predominantly expressed on the vessels with choroidal neovascularization (CNV) but not on normal vessels [43]. However, CCR3 upregulation was not detected in some animal models of CNV [44].

Scg3 was discovered as a highly disease-restricted ligand by comparative ligandomics [13]. Among thousands of quantified endothelial ligands, Scg3 was found with the highest binding activity ratio to diabetic vs. control retinal vessels (1,731:0) and lowest binding to normal vasculature [13]. Indeed, Scg3 stimulated angiogenesis in diabetic but not normal mice. In contrast, VEGF bound to and promoted angiogenesis of both diabetic and control vessels.

In contrast to embryonic lethal $VEGF^{-/+}$ mice, the normal phenotype of $Scg3^{-/-}$ mice implies that Scg3 may not play an important role in vasculogenesis [29, 30], probably because Scg3 receptor is minimally expressed on normal vessels [13, 45]. Given that Scg3 is

constitutively expressed in the normal and OIR retina of neonatal mice, the therapeutic activity of anti-Scg3 mAb implicates that Scg3 is also an OIR-selective angiogenic factor with OIR-induced expression of Scg3 receptor [13]. However, this speculation of Scg3 disease selectivity is yet to be experimentally verified. One of the technical challenges to investigate Scg3 disease selectivity is the unknown identity of Scg3 receptor. Comparative ligandomics is the only approach to quantify its preferential binding to OIR vessels [13].

We recently proposed that therapies targeting highly disease-selective ligands may have the safety advantage with minimal adverse effects on normal cells or vessels [46]. Compared with antibody-drug conjugates (ADCs) for targeted cancer therapy [47], anti-Scg3 mAbs are equivalent to “ligand-guided targeted therapy” without conjugation to a guiding antibody (Fig. 8). This study not only validated Scg3 as a genuine target for anti-angiogenic therapy of OIR but more importantly characterized the safety advantage of targeted anti-Scg3 therapy. Scg3 mAb showed no adverse effect on the developing retinal vasculature (Fig. 5 and Supplementary Fig. 2). ERG was not suppressed by ML78.2 mAb at P21 and P42 (Fig. 4), suggesting that anti-Scg3 therapy should have no short- or long-term adverse effects on retinal development. Systemic safety of anti-Scg3 mAb is also strongly supported by the lack of the adverse effects on body weight gain and kidney, implying that Scg3 inhibitors leaked from the eye will cause minimal safety concern.Optimal safety of anti-Scg3 therapy is also strongly supported by the distinct phenotypes of $Scg3^{-/-}$ and $VEGF^{-/+}$ mice [29, 30]. These findings suggest that anti-Scg3 therapy has the potential to treat not only ROP but also other neonatal angiogenic diseases, such as retinoblastoma in children [48].

Intravitreal injection of anti-VEGF drugs to treat wet AMD and diabetic retinopathy may cause injection-related eye damages, including endophthalmitis, retinal detachment, ocular hemorrhage, increased intraocular pressure and cataract, albeit at a relatively low rate [49, 50]. It is possible that ROP preterm infants are more susceptible to intravitreal injection-related eye injuries than adults. Our results showed that systemic anti-Scg3 mAb is also effective to treat OIR. Because of its high disease selectivity with minimal adverse effects on developing vasculatures and organs, Scg3 inhibitors could be delivered systemically to circumvent intravitreal injection-associated adverse effects. However, the safety of systemic anti-Scg3 Ab to other organs is yet to be thoroughly characterized.

Taken together, this study independently corroborated Scg3 as a genuine target for anti-angiogenic therapy of OIR and demonstrated an optimal safety profile of anti-Scg3 mAbs for ligand-guided targeted therapy (Fig. 8). Anti-Scg3 mAbs with high disease selectivity and safety have the potential to be humanized for clinical therapy of ROP.

Supplementary Material

Refer to Web version on PubMed Central for supplementary material.

Acknowledgements

The authors thank Keith Webster and Philip Rosenfeld for scientific advice and discussion, Rong Wen for instrument support, G. Gaidosh for confocal service, Zhijie Niu for technical support.

Funding

This study was supported by NIH R01EY027749–01A1 (W.L.), R21EY027065 (W.L.), R41EY027665 (W.L. and H.T.), American Diabetes Association 1–18-IBS-172 (W.L.), Special Scholar Award from Research to Prevent Blindness (RPB) (W.L.), the Postgraduate Program of China Scholarships Council #[2016] 3100 (F.T.), American Heart Association Predoctoral Fellowship 14PRE18310014 and 16PRE27250308 (M.E.L), NIH P30-EY014801 and an institutional grant from RPB.

References

1. Chen HX, Cleck JN. Adverse effects of anticancer agents that target the VEGF pathway. Nat Rev Clin Oncol. 2009;6(8):465–77. doi: 10.1038/nrclinonc.2009.94. [PubMed: 19581909]
2. Hellstrom A, Smith LE, Dammann O. Retinopathy of prematurity. Lancet. 2013;382(9902):1445–57. doi: 10.1016/S0140-6736(13)60178-6. [PubMed: 23782686]
3. National Eye Institute. Facts about retinopathy of prematurity (ROP). at https://nei.nih.gov/health/rop/rop.
4. Mantagos IS, Vanderveen DK, Smith LE. Emerging treatments for retinopathy of prematurity. Seminars in ophthalmology. 2009;24(2):82–6. doi: 10.1080/08820530902800322. [PubMed: 19373691]
5. Paulus YM, Sodhi A. Anti-angiogenic Therapy for Retinal Disease. Handb Exp Pharmacol. 2017;242:271–307. doi: 10.1007/164_2016_78. [PubMed: 27783271]
6. Zhang G, Yang M, Zeng J, Vakros G, Su K, Chen M, et al. Comparison of Intravitreal Injection of Ranibizumab Versus Laser Therapy for Zone Ii Treatment-Requiring Retinopathy of Prematurity. Retina. 2017;37(4):710–7. doi: 10.1097/IAE.0000000000001241. [PubMed: 27529839]
7. Mintz-Hittner HA, Kennedy KA, Chuang AZ, Group B-RC. Efficacy of intravitreal bevacizumab for stage 3+ retinopathy of prematurity. N Engl J Med. 2011;364(7):603–15. doi: 10.1056/NEJMoa1007374. [PubMed: 21323540]
8. Mintz-Hittner HA, Geloneck MM, Chuang AZ. Clinical Management of Recurrent Retinopathy of Prematurity after Intravitreal Bevacizumab Monotherapy. Ophthalmology. 2016;123(9):1845–55. doi: 10.1016/j.ophtha.2016.04.028. [PubMed: 27241619]
9. Lepore D, Quinn GE, Molle F, Baldascino A, Orazi L, Sammartino M, et al. Intravitreal bevacizumab versus laser treatment in type 1 retinopathy of prematurity: report on fluorescein angiographic findings. Ophthalmology. 2014;121(11):2212–9. doi: 10.1016/j.ophtha.2014.05.015. [PubMed: 25001158]
10. Jang SY, Choi KS, Lee SJ. Delayed-onset retinal detachment after an intravitreal injection of ranibizumab for zone 1 plus retinopathy of prematurity. J AAPOS. 2010;14(5):457–9. doi: 10.1016/j.jaapos.2010.05.011. [PubMed: 21035077]
11. Tokunaga CC, Mitton KP, Dailey W, Massoll C, Roumayah K, Guzman E, et al. Effects of anti-VEGF treatment on the recovery of the developing retina following oxygen-induced retinopathy. Invest Ophthalmol Vis Sci. 2014;55(3):1884–92. doi: 10.1167/iovs.13-13397. [PubMed: 24550366]
12. Lutty GA, McLeod DS, Bhutto I, Wiegand SJ. Effect of VEGF trap on normal retinal vascular development and oxygen-induced retinopathy in the dog. Invest Ophthalmol Vis Sci. 2011;52(7):4039–47. doi: 10.1167/iovs.10-6798. [PubMed: 21357392]
13. LeBlanc ME, Wang W, Chen X, Caberoy NB, Guo F, Shen C, et al. Secretogranin III as a disease-associated ligand for antiangiogenic therapy of diabetic retinopathy. J Exp Med. 2017;214(4):1029–47. doi: 10.1084/jem.20161802. [PubMed: 28330905]
14. Kim CB, D'Amore PA, Connor KM. Revisiting the mouse model of oxygen-induced retinopathy. Eye Brain. 2016;8:67–79. doi: 10.2147/EB.S94447. [PubMed: 27499653]
15. Wang Z, Raifu M, Howard M, Smith L, Hansen D, Goldsby R, et al. Universal PCR amplification of mouse immunoglobulin gene variable regions: the design of degenerate primers and an assessment of the effect of DNA polymerase 3' to 5' exonuclease activity. J Immunol Methods. 2000;233(1–2):167–77. [PubMed: 10648866]
16. Kim Y, Caberoy NB, Alvarado G, Davis JL, Feuer WJ, Li W. Identification of Hnrph3 as an autoantigen for acute anterior uveitis. Clin Immunol. 2011;138(1):60–6. [PubMed: 20943442]
17. Leenaars M, Hendriksen CF. Critical steps in the production of polyclonal and monoclonal antibodies: evaluation and recommendations. ILAR J. 2005;46(3):269–79. [PubMed: 15953834]

18. Abdiche YN, Miles A, Eckman J, Foletti D, Van Blarcom TJ, Yeung YA, et al. High-throughput epitope binning assays on label-free array-based biosensors can yield exquisite epitope discrimination that facilitates the selection of monoclonal antibodies with functional activity. PLoS One. 2014;9(3):e92451. doi: 10.1371/journal.pone.0092451. [PubMed: 24651868]
19. Estep P, Reid F, Nauman C, Liu Y, Sun T, Sun J, et al. High throughput solution-based measurement of antibody-antigen affinity and epitope binning. mAbs. 2013;5(2):270–8. doi: 10.4161/mabs.23049. [PubMed: 23575269]
20. Barbas CF 3rd, Kang AS, Lerner RA, Benkovic SJ. Assembly of combinatorial antibody libraries on phage surfaces: the gene III site. Proc Natl Acad Sci U S A. 1991;88(18):7978–82. [PubMed: 1896445]
21. Barbas CF 3rd, Burton DR, Scott JK, Silverman GJ. Phage display: a laboratory manual. 2000;Cold Spring Harbor Laboratory Press, Cold Spring Harbor, New York.
22. Li W, Handschumacher RE. Identification of two calcineurin B-binding proteins: tubulin and heat shock protein 60. Biochim Biophys Acta. 2002;1599(1–2):72–81. [PubMed: 12479407]
23. Caberoy NB, Zhou Y, Jiang X, Alvarado G, Li W. Efficient identification of tubby-binding proteins by an improved system of T7 phage display. J Mol Recognit. 2010;23(1):74–83. [PubMed: 19718693]
24. Connor KM, Krah NM, Dennison RJ, Aderman CM, Chen J, Guerin KI, et al. Quantification of oxygen-induced retinopathy in the mouse: a model of vessel loss, vessel regrowth and pathological angiogenesis. Nat Protoc. 2009;4(11):1565–73. doi: 10.1038/nprot.2009.187. [PubMed: 19816419]
25. Li W, Krasinski SD, Verhave M, Montgomery RK, Grand RJ. Three distinct messenger RNA distribution patterns in human jejunal enterocytes. Gastroenterology. 1998;115(1):86–92. [PubMed: 9649462]
26. Kurus M, Ugras M, Esrefoglu M. Effect of resveratrol on tubular damage and interstitial fibrosis in kidneys of rats exposed to cigarette smoke. Toxicol Ind Health. 2009;25(8):539–44. doi: 10.1177/0748233709346755. [PubMed: 19825860]
27. Toledo-Rodriguez M, Loyse N, Bourdon C, Arab S, Pausova Z. Effect of prenatal exposure to nicotine on kidney glomerular mass and AT1R expression in genetically diverse strains of rats. Toxicol Lett. 2012;213(2):228–34. doi: 10.1016/j.toxlet.2012.06.009. [PubMed: 22728133]
28. Sapieha P Eyeing central neurons in vascular growth and reparative angiogenesis. Blood. 2012;120(11):2182–94. doi: 10.1182/blood-2012-04-396846. [PubMed: 22705597]
29. Ferrara N, Carver-Moore K, Chen H, Dowd M, Lu L, O'Shea KS, et al. Heterozygous embryonic lethality induced by targeted inactivation of the VEGF gene. Nature. 1996;380(6573):439–42. doi: 10.1038/380439a0. [PubMed: 8602242]
30. Kingsley DM, Rinchik EM, Russell LB, Ottiger HP, Sutcliffe JG, Copeland NG, et al. Genetic ablation of a mouse gene expressed specifically in brain. EMBO J. 1990;9(2):395–9. [PubMed: 2303033]
31. Wu WC, Lien R, Liao PJ, Wang NK, Chen YP, Chao AN, et al. Serum levels of vascular endothelial growth factor and related factors after intravitreous bevacizumab injection for retinopathy of prematurity. JAMA Ophthalmol. 2015;133(4):391–7. doi: 10.1001/jamaophthalmol.2014.5373. [PubMed: 25569026]
32. Sato T, Wada K, Arahori H, Kuno N, Imoto K, Iwahashi-Shima C, et al. Serum concentrations of bevacizumab (avastin) and vascular endothelial growth factor in infants with retinopathy of prematurity. Am J Ophthalmol. 2012;153(2):327–33 el. doi: 10.1016/j.ajo.2011.07.005. [PubMed: 21930258]
33. Kandasamy Y, Hartley L, Rudd D, Smith R. The association between systemic vascular endothelial growth factor and retinopathy of prematurity in premature infants: a systematic review. Br J Ophthalmol. 2017;101(1):21–4. doi: 10.1136/bjophthalmol-2016-308828. [PubMed: 27388246]
34. Darlow BA, Ells AL, Gilbert CE, Gole GA, Quinn GE. Are we there yet? Bevacizumab therapy for retinopathy of prematurity. Arch Dis Child Fetal Neonatal Ed. 2013;98(2):F170–4. doi: 10.1136/archdischild-2011-301148. [PubMed: 22209748]

35. McGrath-Morrow S, Cho C, Molls R, Burne-Taney M, Haas M, Hicklin DJ, et al. VEGF receptor 2 blockade leads to renal cyst formation in mice. Kidney Int. 2006;69(10):1741–8 doi: 10.1038/sj.ki.5000314. [PubMed: 16572116]
36. Rosenstein JM, Mani N, Khaibullina A, Krum JM. Neurotrophic effects of vascular endothelial growth factor on organotypic cortical explants and primary cortical neurons. J Neurosci. 2003;23(35):11036–44. [PubMed: 14657160]
37. Atchaneeyasakul LO, Trinavarat A. Choroidal ruptures after adjuvant intravitreal injection of bevacizumab for aggressive posterior retinopathy of prematurity. J Perinatol. 2010;30(7):497–9. doi: 10.1038/jp.2009.166. [PubMed: 20585321]
38. Wu WC, Yeh PT, Chen SN, Yang CM, Lai CC, Kuo HK. Effects and complications of bevacizumab use in patients with retinopathy of prematurity: a multicenter study in taiwan. Ophthalmology. 2011;118(1):176–83. doi: 10.1016/j.ophtha.2010.04.018. [PubMed: 20673589]
39. Suk KK, Berrocal AM, Murray TG, Rich R, Major JC, Hess D, et al. Retinal detachment despite aggressive management of aggressive posterior retinopathy of prematurity. J Pediatr Ophthalmol Strabismus. 2010;47 Online:e1–4. doi: 10.3928/01913913-20101217-06.
40. Geloneck MM, Chuang AZ, Clark WL, Hunt MG, Norman AA, Packwood EA, et al. Refractive outcomes following bevacizumab monotherapy compared with conventional laser treatment: a randomized clinical trial. JAMA Ophthalmol. 2014;132(11):1327–33. doi: 10.1001/jamaophthalmol.2014.2772. [PubMed: 25103848]
41. Autrata R, Krejcirova I, Senkova K, Holousova M, Dolezel Z, Borek I. Intravitreal pegaptanib combined with diode laser therapy for stage 3+ retinopathy of prematurity in zone I and posterior zone II. Eur J Ophthalmol. 2012;22(5):687–94. doi: 10.5301/ejo.5000166. [PubMed: 22669848]
42. Al-Hilal TA, Chung SW, Choi JU, Alam F, Park J, Kim SW, et al. Targeting prion-like protein doppel selectively suppresses tumor angiogenesis. J Clin Invest. 2016;126(4):1251–66. doi: 10.1172/JCI83427. [PubMed: 26950422]
43. Takeda A, Baffi JZ, Kleinman ME, Cho WG, Nozaki M, Yamada K, et al. CCR3 is a target for age-related macular degeneration diagnosis and therapy. Nature. 2009;460(7252):225–30. doi: 10.1038/nature08151. [PubMed: 19525930]
44. Li Y, Huang D, Xia X, Wang Z, Luo L, Wen R. CCR3 and choroidal neovascularization. PLoS One. 2011;6(2):e17106. doi: 10.1371/journal.pone.0017106. [PubMed: 21358803]
45. Ottiger HP, Battenberg EF, Tsou AP, Bloom FE, Sutcliffe JG. 1B1075: a brain- and pituitary-specific mRNA that encodes a novel chromogranin/secretogranin-like component of intracellular vesicles. J Neurosci. 1990;10(9):3135–47. [PubMed: 2204688]
46. Li W, Pang IH, Pacheco MTF, Tian H. Ligandomics: a paradigm shift in biological drug discovery. Drug Discov Today. 2018;23(3):636–43. doi: 10.1016/j.drudis.2018.01.013. [PubMed: 29326083]
47. Sau S, Alsaab HO, Kashaw SK, Tatiparti K, Iyer AK. Advances in antibody-drug conjugates: A new era of targeted cancer therapy. Drug Discov Today. 2017;22(10):1547–56. doi: 10.1016/j.drudis.2017.05.011. [PubMed: 28627385]
48. de Aguirre Neto JC, Antoneli CB, Ribeiro KB, Castilho MS, Novaes PE, Chojniak MM, et al. Retinoblastoma in children older than 5 years of age. Pediatr Blood Cancer. 2007;48(3):292–5. doi: 10.1002/pbc.20931. [PubMed: 16847922]
49. Dedania VS, Bakri SJ. Current perspectives on ranibizumab. Clin Ophthalmol. 2015;9:533–42. doi: 10.2147/OPTH.S80049. [PubMed: 25848203]
50. Drug_Information. Lucentis prescribing information by U.S. Food and Drug Administration at http://www.accessdata.fda.gov/drugsatfda_docs/label/2006/125156lbl.pdf.

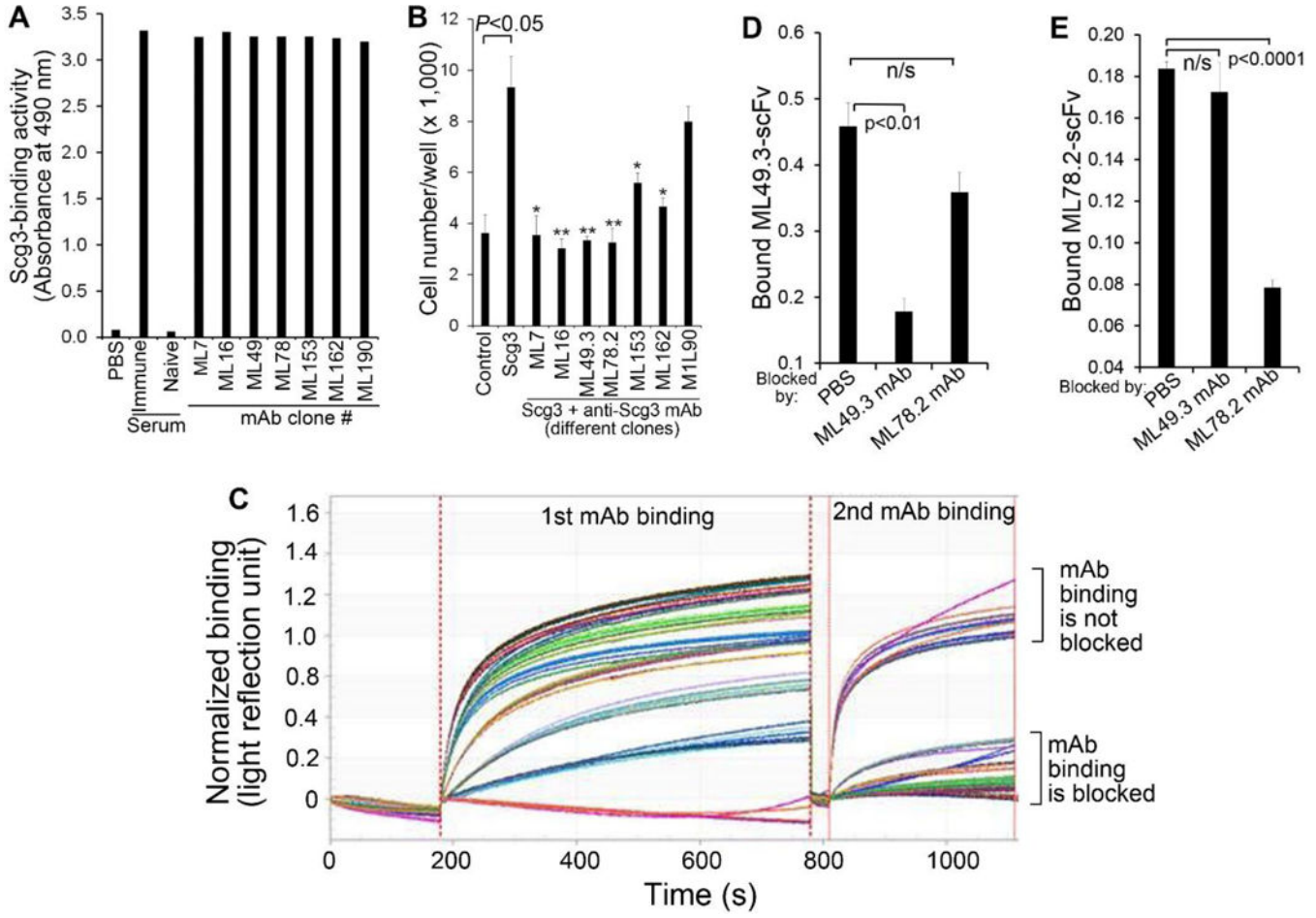

Fig. 1.

ML78.2 and ML49.3 mAbs are non-competing Scg3-neutralizing antibodies. **a** Seven independent clones of anti-Scg3 mAbs were analyzed for their binding activity to immobilized Scg3 by ELISA assay. n=3 wells. **b** Six out of seven anti-Scg3 mAbs are capable of neutralizing Scg3-induced proliferation of HUVECs. n=3 wells. * p<0.05, ** p<0.01. **c** Epitope binning of seven clonal anti-Scg3 mAbs using Octet RED96. Biotin-labeled Scg3 was immobilized on streptavidin biosensors for mAb binding detection twice. The 1st bound mAbs served as blockers to the 2nd mAbs. ML49.3 and ML78.2 were characterized as non-competing mAbs. **d** ELISA assay to confirm that ML49.3 scFv binding to immobilized Scg3 was blocked by ML49.3 mAb but not ML78.2 mAb. n=3 wells. **e** ELISA assay to verify ML78.2 scFv binding to Scg3 was blocked by ML78.2 mAb, but not ML49.3 mAb. n=3 wells. ± SEM; one-way ANOVAtest.

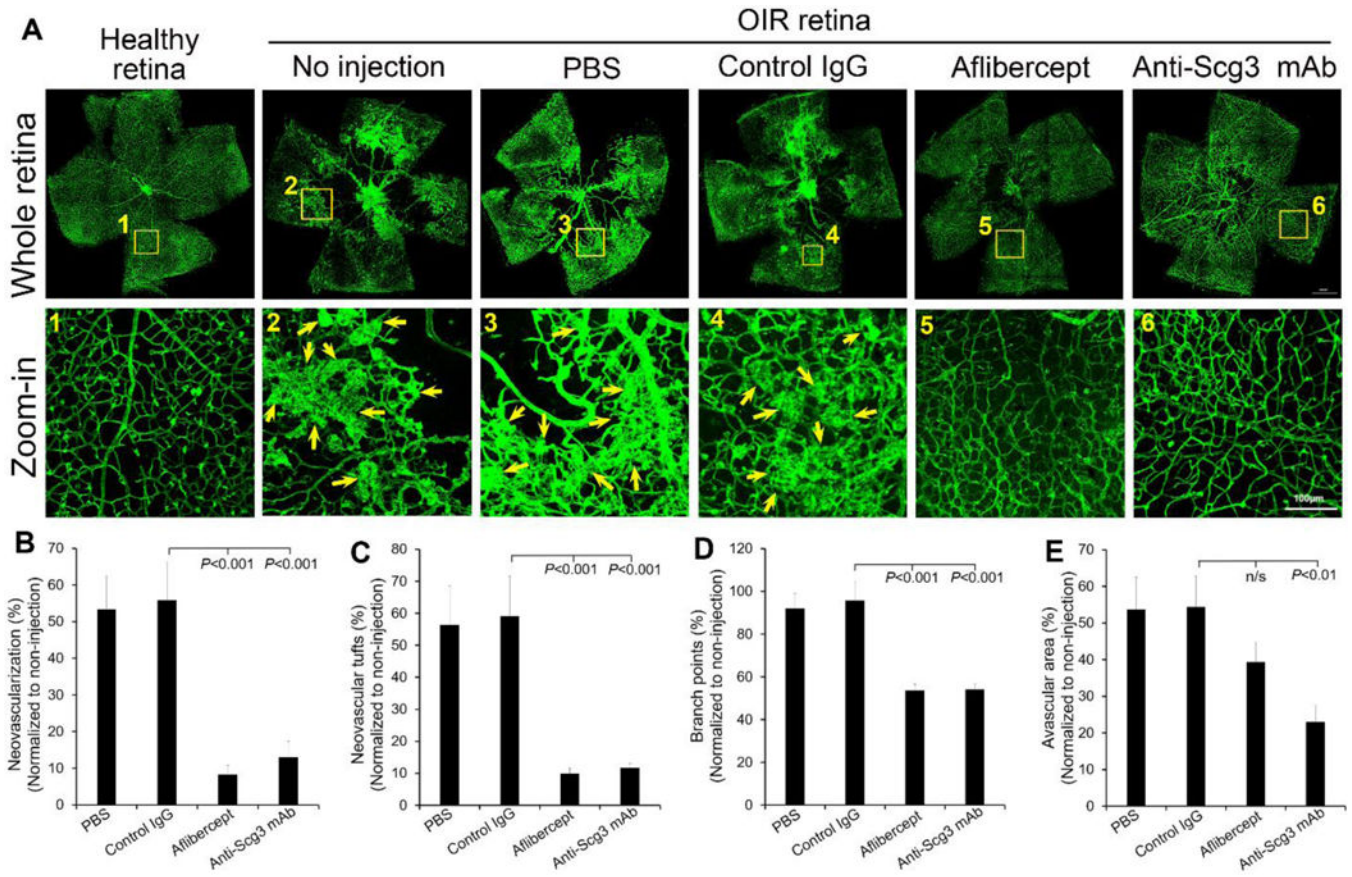

Fig. 2.

Anti-Scg3 mAb to treat OIR via intravitreal injection. Anti-Scg3 ML78.2 mAb (4 μg/eye), control mouse IgG1, aflibercept (2 μg/eye) or PBS was injected at P14. **a** Representative images of flat-mount OIR retina. Arrows indicate neovascularization and NV tufts. **b** Retinal neovascularization. **c** NV tufts. **d** Branch points. e Avascular area. n= 10 eyes (PBS), n= 7 eyes (control IgG), n=11 eyes (aflibercept), n= 9 eyes (anti-Scg3 mAb). Bar = 100 μm (zoom-in). ± SEM, one-way ANOVAtest.

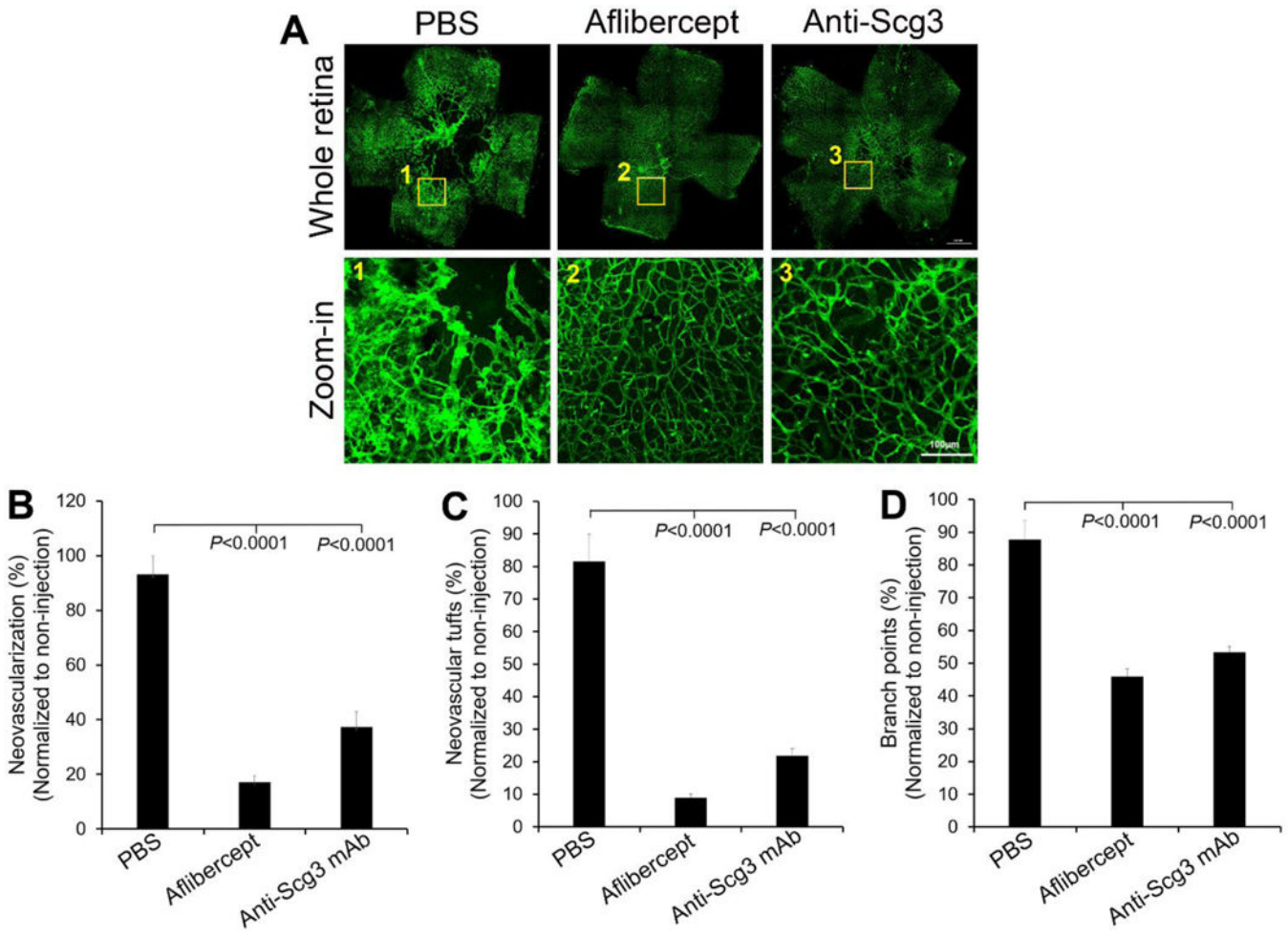

Fig. 3.

Anti-Scg3 mAb to treat OIR via intraperitoneal injection. Therapeutic agents were injected at P14. **a** Representative images of OIR retina. **b** Retinal neovascularization. **c** NV tufts. **d** branch points. Bar = 100 μm (zoom-in). n= 8 eyes (PBS), n= 13 eyes (aflibercept), n= 15 eyes (anti-Scg3 mAb). ± SEM, one-way ANOVA test.

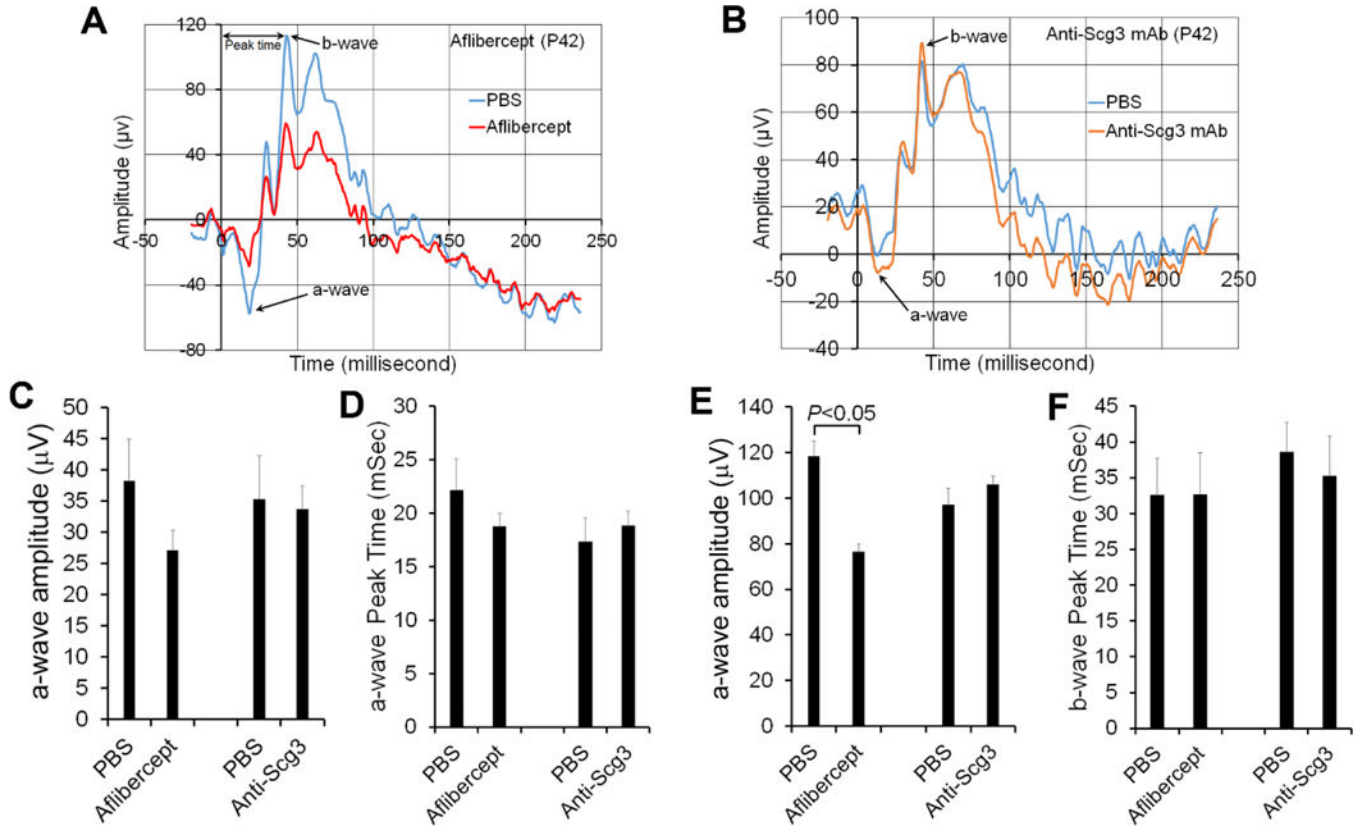

Fig. 4.

Anti-Scg3 mAb has minimal adverse effects on retinal function after intravitreal injection. Anti-Scg3 mAb or aflibercept (4 μg/eye) was intravitreally injected into mice at P14 with PBS for the fellow eye. ERG was performed at P21 (not shown) and P42. **a** Representative ERG of aflibercept-treated eye at P42. **b** Representative ERG of anti-Scg3 mAb-treated eye at P42. **c** Amplitude of a-wave at P42. **d** Latency of a-wave at P42. **e** Amplitude of b-wave at P42. **f** Latency of b-wave at P42. ± SEM, n=6 mice, paired *t*-test.

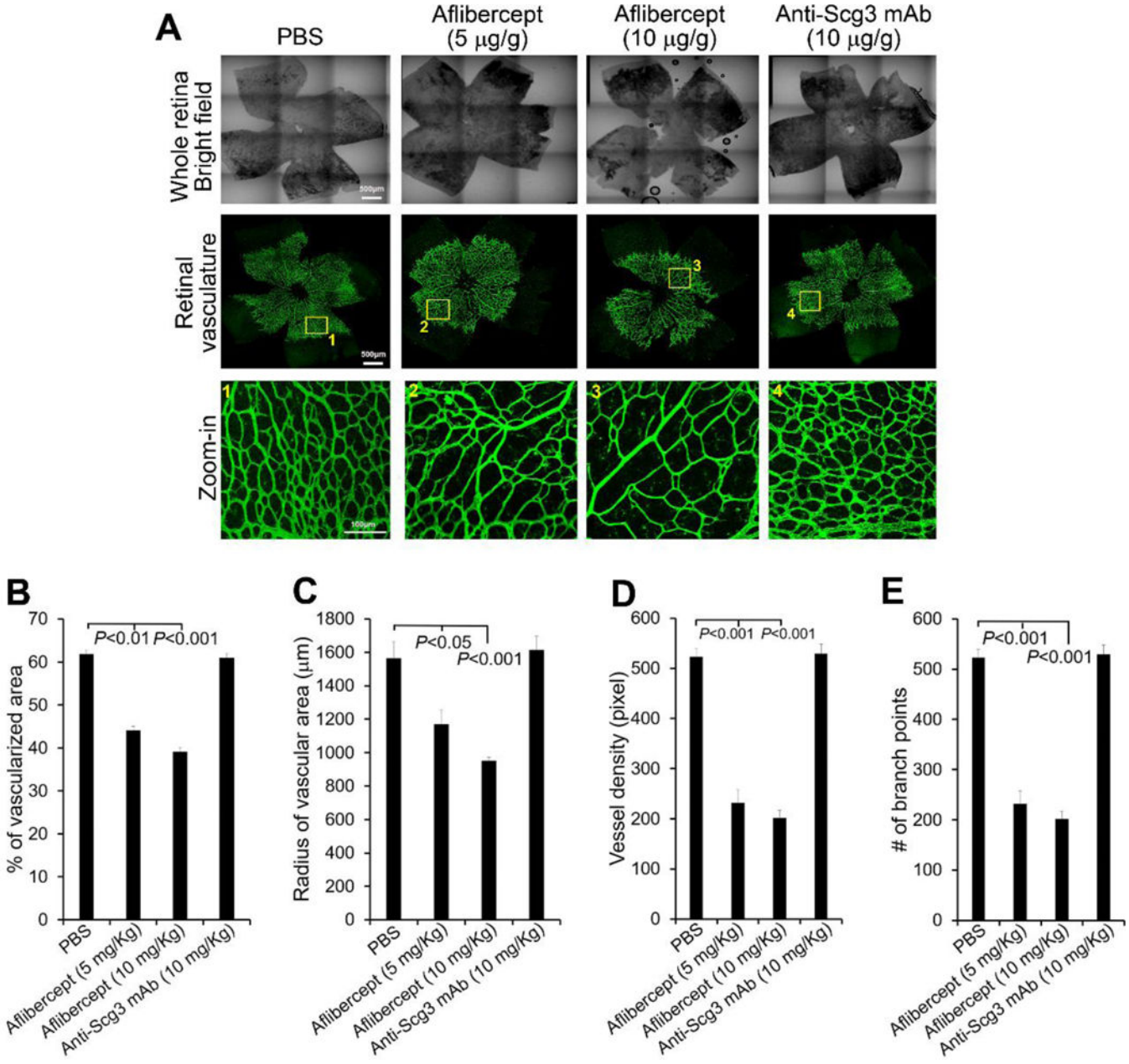

Fig. 5.

Aflibercept, but not anti-Scg3 mAb, suppresses the development of retinal vasculature at P6. Aflibercept (5 or 10 mg/Kg body weight) or anti-Scg3 ML78.2 mAb (10 mg/Kg) were injected i.p. into mice at P1, 3 and 5. At P6, retinas were isolated, stained with fluorescent isolectin B4, analyzed by confocal microscopy. **a** Representative images of retinas in the bright and fluorescent fields. Bar= 500 μm (top two rows), 100 μm (bottom row). **b** Percentage of vascularized area. **c** Radius of vascularized retina. **d** Branch points. **e** Vessel density. n=5 eyes (PBS), 6 eyes (aflibercept 5 or 10 mg/Kg), n= 4 eyes (anti-Scg3 mAb). ± SEM, one-way ANOVA test.

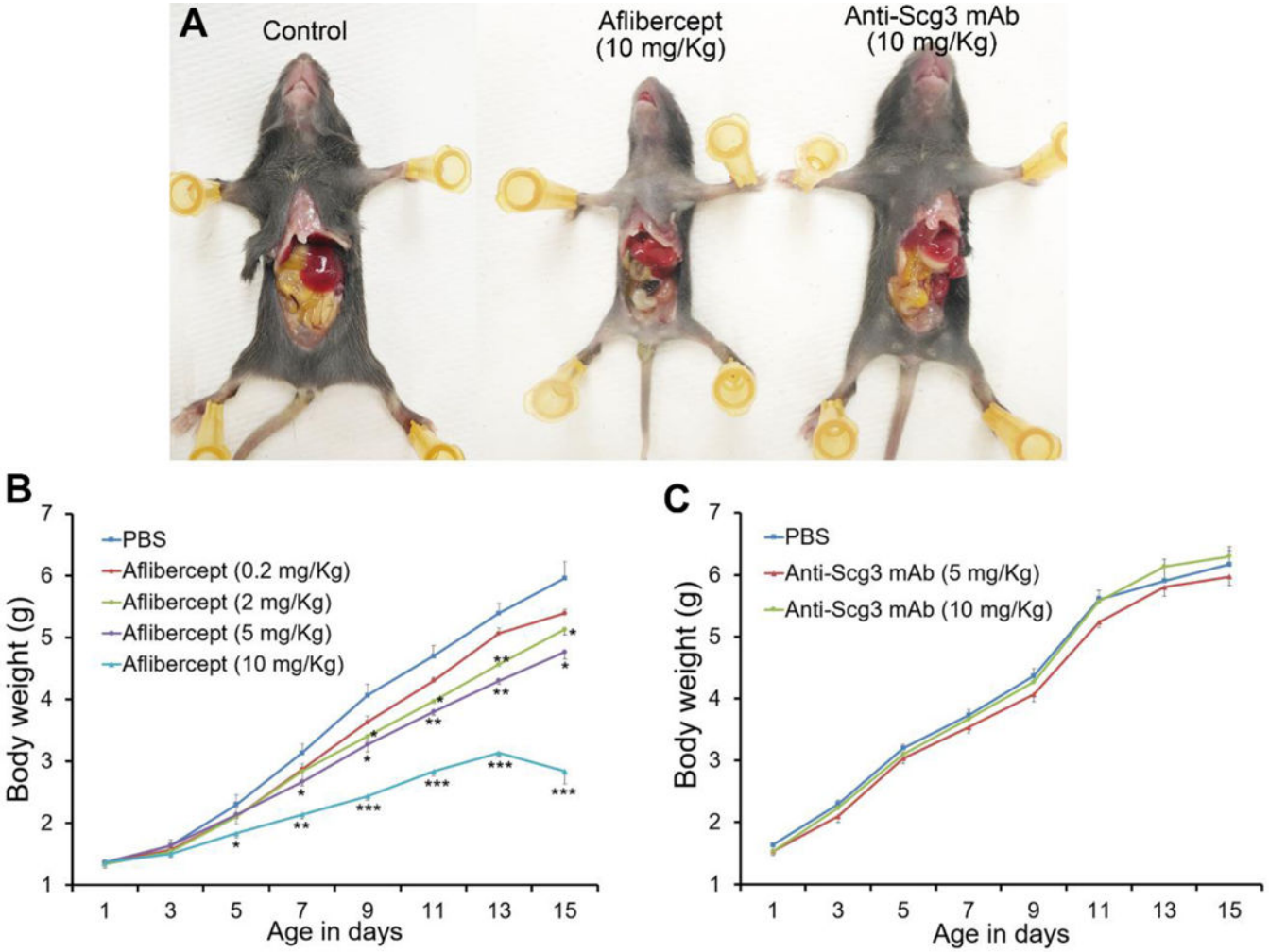

Fig. 6.

Aflibercept, but not anti-Scg3 mAb, retards body weight gain in neonatal mice. Anti-Scg3 ML78.2 mAb or aflibercept was i.p. injected to mice at P3, 5, 7, 9, 11 and 13. **a** Representative images of mouse size. **b** Body weight of aflibercept-treated mice. **c** Body weight of anti-Scg3 mAb-treated mice. n=3 mice, ±SEM, one-way ANOVA test.

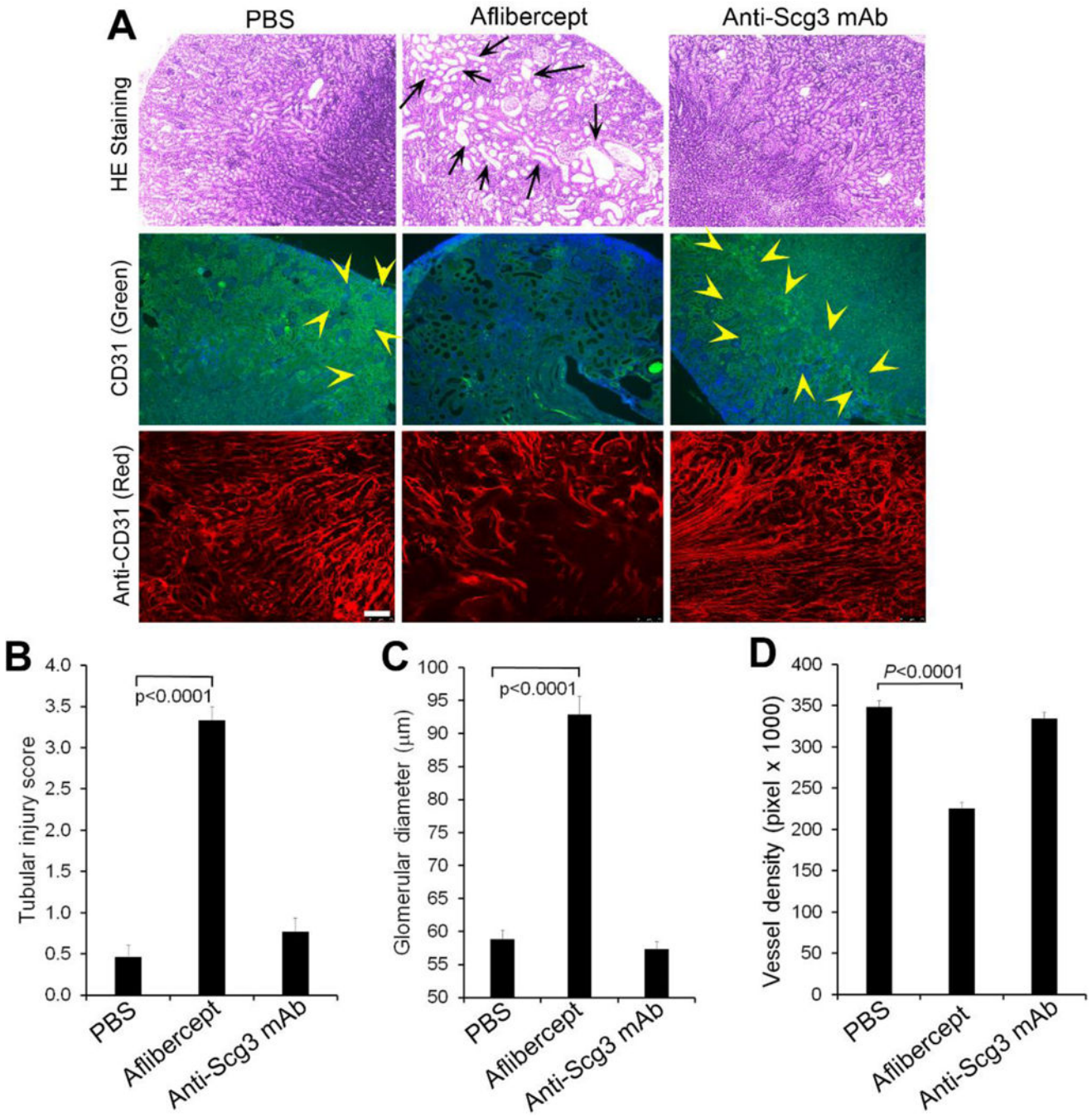

Fig. 7.

Anti-Scg3 mAb has no adverse on the developing kidney. Anti-Scg3 ML78.3 mAb or aflibercept (10 mg/Kg body weight) was injected i.p. into mice at P3, 5, 7, 9, 11 and 13. Kidneys were isolated at P15 and stained with H&E or anti-CD31 mAb. **a** Representative image of kidney H&E or CD31 Ab staining. Top row: H&E staining. Middle row: FITC-anti-CD31 mAb. Bottom row: Alexa Fluor 594-anti-CD31 mAb. Arrows indicate dilated tubules. Arrowheads indicate CD31-positive signals. **b** Quantification of tubular injury. **c** Quantification of glomerular dimeter. n=13 (PBS and anti-Scg3 mAb) and 16 (aflibercept).

d Quantification of vessel density labeled with Alexa Fluor 594-anti-CD31 mAb. Bar=75 μm. n=8, ± SEM, one-way ANOVA test.

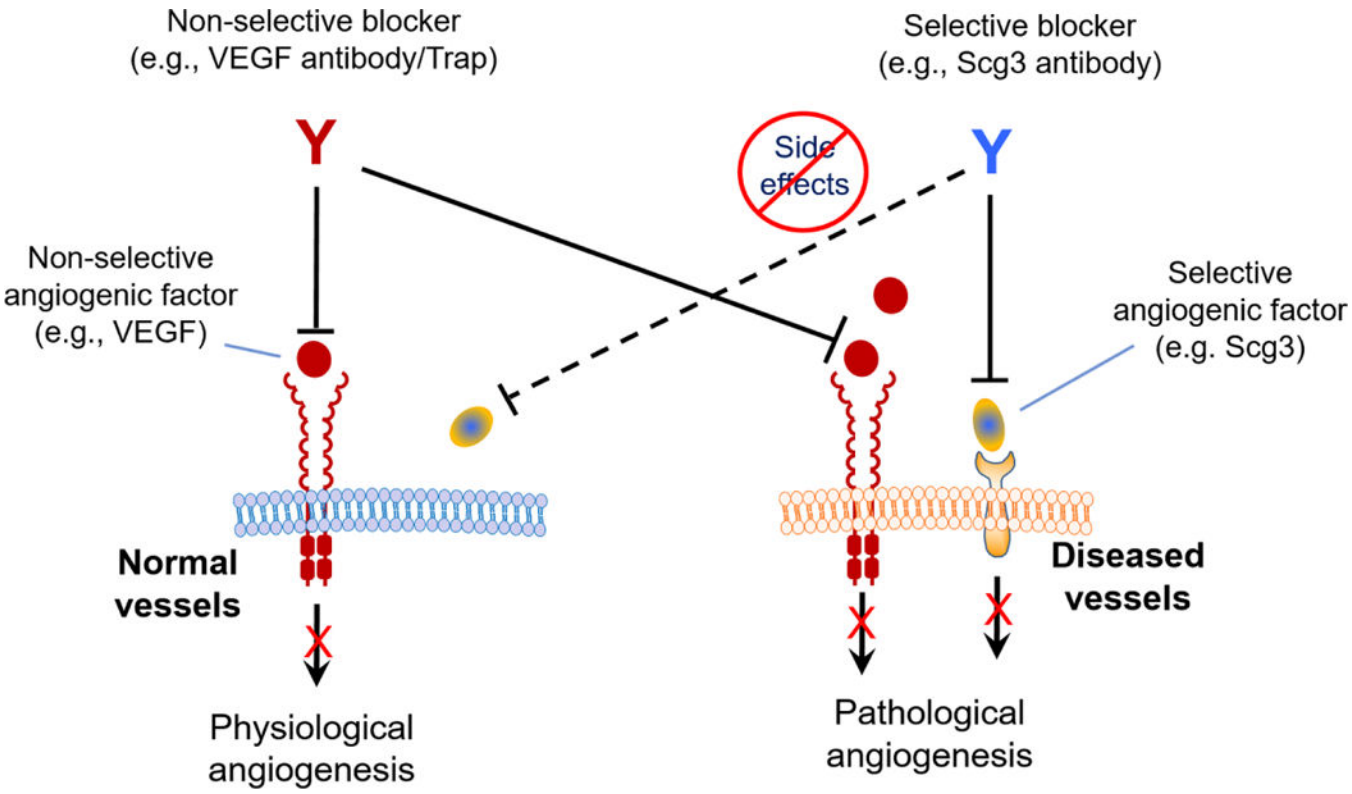

Fig. 8.

Ligand-guided targeted anti-angiogenic therapy. VEGF regulates both diseased and healthy vessels, whereas Scg3 binds only to diseased but not normal vasculatures. Anti-VEGF drugs blocks pathological and physiological angiogenesis. In contrast, anti-Scg3 mAb selectively inhibits pathological but not physiological angiogenesis.